J Inorg Organomet Polym (2012) 22:1254–1262
DOI 10.1007/s10904-012-9734-4

Development and Characterization of Curcumin Loaded Silver Nanoparticle Hydrogels for Antibacterial and Drug Delivery Applications

Sakey Ravindra · Antoine F. Mulaba-Bafubiandi · V. Rajinikanth · K. Varaprasad · N. Narayana Reddy · K. Mohana Raju

Received: 11 May 2012 / Accepted: 31 July 2012 / Published online: 14 August 2012

Abstract The present work involves the development of curcumin loaded silver hydrogel nanocomposites based on acrylamide and 2-acrylamido-2-methyl propanesulfonic acid, as a template by redox co-polymerization in the presence of hydrophilic crosslinker *N*,*N*^{1}-methylenebisacrylamide. Silver nitrate was taken as the metal precursor and sodium borohydride as a reducing agent. The formation of silver nanoparticles was monitored using UV–Vis absorption spectroscopy. The developed hydrogel silver nanocomposites (HSNC) were characterized by FTIR, UV–Vis, thermogravimetric analysis, scanning electron microscopy and transmission electron microscopy. The curcumin loading and release characteristics were performed for different hydrogel systems. The developed HSNCs were evaluated for preliminary antibacterial applications.

Keywords Hydrogel network · Silver nanoparticles · Antibacterial activity

S. Ravindra (✉)
Department of Chemical Engineering Technology, Faculty of Engineering and the Built Environment, University of Johannesburg, Doornfontein Campus, P.O. Box 17011, Johannesburg 2028, South Africa
e-mail: ravisakey@gmail.com

A. F. Mulaba-Bafubiandi · V. Rajinikanth
Department of Metallurgy, Faculty of Engineering and the Built Environment, University of Johannesburg, P.O. Box 526, Johannesburg 2028, South Africa

K. Varaprasad · K. Mohana Raju
Synthetic Polymer Laboratory, Department of Polymer Science & Technology, Sri Krishnadevaraya University, Anantapur 515055, India

N. Narayana Reddy
Department of General, Organic and Biomedical Chemistry, University of Mons, Mons, Belgium

1 Introduction

Over the past few years, majority of the colloidal researchers have shifted their focus from micrometer-size particles to nanometer-sized particles. Particular focus was on metal nanoparticles (e.g.; silver, copper and gold) because of their ease of fabrication and their strong optical absorbencies [1–3]. During the past few years silver nanoparticles have demonstrated significant antimicrobial effect to fight against infection and diseases [4]. The application of colloidal silver nanoparticles depends on the colloidal stability of the particles. To achieve this, colloidal silver nanoparticles are coated with organic molecules, inorganic material or polymers to facilitate their use in catalysis, optics, electronics and antimicrobial activity [5–8]. Generally, metal nanoparticles are prepared and stabilized by physical and chemical methods; the chemical approach including chemical reduction, electrochemical techniques, and photochemical reduction is most widely used. Among these, chemical reductions is the most frequently applied method for the preparation of silver nanoparticles (AgNPs) as stable, colloidal dispersions in water or organic solvents [9–15]. These stabilized silver nanoparticles have been applied to a wide range of healthcare products such as burn dressings, scaffold, skin donor and recipient sites, water purification systems and medical devices [16–20]. Electhiguerra et al. [21] demonstrated that silver nanoparticles undergo a size-dependent interaction with HIV-1 virus via preferential binding to the gp120 glycoprotein knobs, thus the inhibiting the virus from binding to the host cells. The most advanced feature of this novel approach is that one can alter the size and morphology of the nanoparticles by changing the monomer and crosslinker concentrations in the gel formulations. Well defined gold nanoparticles embedded inside thermo sensitive hydrogel matrices were reported by Wang et al. [22, 23]. In their

network, the templates of the gel networks were prepared using a combination of two crosslinkers, namely *N*,*N*-methylenebisacrylamide (MBA) and *N*,*N*-cystaminebisacrelamide (CBA). CBA is highly responsible in controlling the morphology of the nanoparticles by controlling the crosslinking density of the networks. In another study, silver nanoparticles of ~35 nm are embedded in a novel hydrogel system based on poly(vinyl alcohol)/poly(styrene)-co-poly(ethylene glycol methacrylate) (PVA/PS-PEGMA) [24]. Saravanan et al. [25] has shown that poly(acrylamide) hydrogels are effective for the production of nano-sized silver particles (~4 nm). All the above hydrogel-nanoparticle composites are based on silver nanoparticles only because of their exponential use in the treatments of infections in burns, traumatic wounds and diabetic ulcers [26].

A number of antibacterial materials (Nanosilver: Nano-CET, Mumbai, India, IonAumour: IONAURMOUR, Philadelphia, PA) are commercially available. These nanosilver products are embedded in some polymer matrices or composite materials but the release of AgNP is not in a sustained manner. This paper reports on the development of silver nanoparticles loaded in hydrogels. Curcumin (CUR) is a hydrophobic polyphenolic compound derived from the rhizome of the herb *Curcuma longa*, possesses a wide range of biological activities including wound healing, anti-bacterial, anti-oxidant, anti-inflammatory and anti-cancer properties [27].

To achieve novel and better antibacterial products, hydrogel-silver nanoparticle-curcumin composites are developed in the present investigation. For obtaining these products, poly(Am-co-Amps) hydrogels are synthesized. We also evaluate the curcumin loading and release characteristics for these hydrogel systems.

2 Materials

Acrylamide (AM), ammonium persulfate (APS), MBA, silver nitrate ($AgNO_3$), sodium borohydride ($NaBH_4$) were purchased from S D Fine Chemicals (Mumbai, India). 2-acrylamido-2-methyl propanesulfonic acid (AMPS) was purchased from Merck. (Bombay, India). *N,N,N*^{1},*N*^{1}-tetramethylethylenediamine (TMEDA) was purchased from Aldrich Chemical Company Inc. (Milwaukee, WI, USA). Curcumin is a gift sample from M/s Natural Remedies Pvt. Ltd. (Bangalore, India). All the chemicals were used with out further purification. Double distilled (DB) water was used throughout the investigations.

2.1 Preparation of Poly(AM-co-AMPS) Hydrogels

The hydrogels were prepared using free radical copolymerization of AM and AMPS using MBA as the crosslinker, and APS/TMEDA as the initiating system. Polymerizations were performed in 100 ml beakers at room temperature. In order to finalize an optimized hydrogel, a series of poly (Am-Amps) hydrogels were synthesized by varying the different reaction parameters. The feed composition for the all the gels are indicated in Table 1.

2.2 Preparation of Poly(AM-co-AMPS)hydrogel-Silver Nanocomposites

To prepare hydrogel-silver nanocomposites, accurately weighed dry hydrogels were equilibrated with water for 3 days and these hydrogels were transferred to a beaker containing 50 ml of 5 mM $AgNO_3$ aqueous solution, allowed to equilibrate for 1 day. During these, the silver ions are being exchanged from solution to the gel networks. These silver salt loaded hydrogels were finally transferred into a beaker containing 50 ml of 10 mM $NaBH_4$ aqueous solution and allowed for 2 h to reduce the silver ions into silver nanoparticles. The obtained silver nanoparticles in the hydrogels are often termed in the forth coming sections as hydrogel-silver nanocomposites (HSNC).

The prepared hydrogels with different concentrations of AMPS and MBA were employed for producing the HSNC. The resulting nanocomposite is termed HSNC–AMPS and HSNC–MBA.

2.3 Curcumin Loaded Hydrogels

The loading of Curcumin into hydrogels was conducted by swelling equilibrium method. 50 mg of hydrogels are allowed to swell in 20 ml of curcumin solution (5 mg/20 ml, 4:6 acetone:distilled water) for 24 h at 25 °C in the dark (because curcumin is photosensitive). Then, the hydrogel was taken out from the curcumin solution and washed with

Table 1 Preparation conditions of poly(AM-co-AMPS) hydrogels

Hydrogel codes	AMPS (gm)	MBA (mM)
PAM	–	0.648
PAM-A1	0.1	0.648
PAM-A2	0.2	0.648
PAM-A3	0.3	0.648
PAM-A4	0.4	0.648
PAM-A5	0.5	0.648
PAM-M1	0.3	1.94
PAM-M2	0.3	3.24
PAM-M3	0.3	4.54
PAM-M4	0.3	7.78
PAM-M5	0.3	9.72

AM (14.26 mM); APS (2.18 mM); TMEDA (0.86 mM); temperature, 28 ± 1 °C; 24 h

20 ml of water (three times) to remove the excess of curcumin present on the surface of the hydrogel. Finally, these gels are dried at 25 °C in the dark for 48 h to obtain the release device. Drug encapsulation efficiency was calculated by using the remaining amount of curcumin solution after hydrogel loading was done. After removing the hydrogel from the curcumin solution, the remaining drug solution was analyzed by using Elico SL164 UV spectrophotometer (The Science House, Hyderabad, India) at λ_{max} 491.2 nm. The loading efficiency of curcumin in the hydrogels is monitored spectrophotometrically [28]. The curcumin-loaded hydrogels are placed in 50 ml of buffer solution (pH 7.4) and stirred vigorously for 160 h to extract the curcumin from the hydrogels. The solution is filtered and assayed by using UV spectrophotometer at a fixed λ_{max} value of 491.2 nm. The results of % drug loading and encapsulation efficiency are calculated using the following equations.

$$\% \text{ Drug loading} = \left[\text{weight of drug in the hydrogel} / \text{weight of hydrogel}\right] \times 100$$

$$\% \text{ Encapsulation efficiency} = [\% \text{ actual loading} / \% \text{ theoretical loading}] \times 100$$

2.4 Swelling Studies

Completely dried hydrogels and hydrogel nanocomposites were equilibrated in water for 3 days at 30 °C. The swelling ratio (Q) of the gels was calculated from the following equation

$$Q = W_e / W_d$$

where W_e is the weight of the water in the swollen hydrogel and W_d is the dry weight of the pure hydrogel.

Similarly by employing the same method swelling studies of these hydrogels in biological fluids (PECF solution) were evaluated. The biological fluid consists of 0.68 g of NaCl, 0.22 g of KCl, 2.5 g of $NaHCO_3$ and 0.35 g of NaH_2PO_4 in 100 ml of distilled water [29]. Hydrogels were perfectly weighed and then soaked in PECF solution at same condition. After equilibrium swelling, they removed from solvent carefully and wiped by filter papers, weighed, and placed in PECF solution. This procedure was repeated several times until a constant weight was reached for each sample. The swelling ratio (g/g) of hydrogels was calculated from the final weight of the hydrogel divided by the initial weight of the sample.

2.5 Characterization

FTIR spectra of hydrogel and HSNC were recorded with a Thermo Nicolet Nexus 670 spectrophotometer (Washington, USA). UV–Vis spectra of IHSNC (10 mg in 1 ml of distilled water) were carried out on a Elico SL164UV spectrophotometer (The Science House, Hyderabad, India). The thermal stabilities of these nanocomposites were evaluated using Mettler Toledo 851e thermal system (Zurich, Switzerland) at a heating rate of 10 °C/min under nitrogen atmosphere (flow rate, 10 ml/min. Scanning electron microscope (SEM) images was taken with a Hitachi S-4700 (Japan) operating at an acceleration voltage of 15 kV. The sizing of the samples was carried out from transmission electron micrograph using a Tecnai F 12 transmission electron microscope (TEM) operating at an acceleration voltage of 15 kV. For TEM measurements, samples were prepared by dropping 10–20 µl of finely grinded HSNC dispersions on a copper grid and dried at room temperature after removing excess solution using filter paper.

2.6 Release of Curcumin

In order to study the release pattern of curcumin from the loaded hydrogels, a known weight of curcumin loaded hydrogel is placed in 50 ml of 7.4 pH phosphate buffer at 37 °C temperature. The released amount of curcumin is determined at different time intervals by recording the absorbance of the release medium by using UV–Vis spectrophotometer ELICO SL 164 Model (The Elico Co, Hyderabad, India). The absorption of the solutions is measured at λ_{max} 491.2 nm.

2.7 Antibacterial Activity

The antibacterial activity of the developed samples was tested against *E. coli*. The nutrient agar medium was prepared by using peptone (5.0 g), beef extract (3.0 g), and sodium chloride (NaCl) (5.0 g) in 1,000 ml distilled water and the pH was adjusted to 7.0 and agar (15.0 g) was added to this solution. The agar medium was sterilized in a conical flask at a pressure of 15 lbs for 30 min. This nutrient agar medium was transferred into sterilized petri dishes in a laminar air flow. After solidification of the media, *E. coli* culture was streaked on the solid surface of the media. To this inoculated petri dish, one drop of gel particle solution (20 mg/10 ml distilled water) was added using 50-µl tip and incubated for 2 days at 37 °C in the incubation chamber.

3 Results and Discussion

During the past few years, a number of different approaches have been used to obtain better stabilization of nanoparticles using various polymers, block copolymers, dendrimers, microgels, and hydrogels and so on. There is a lot of interest in producing nanoparticles in the hydrogel

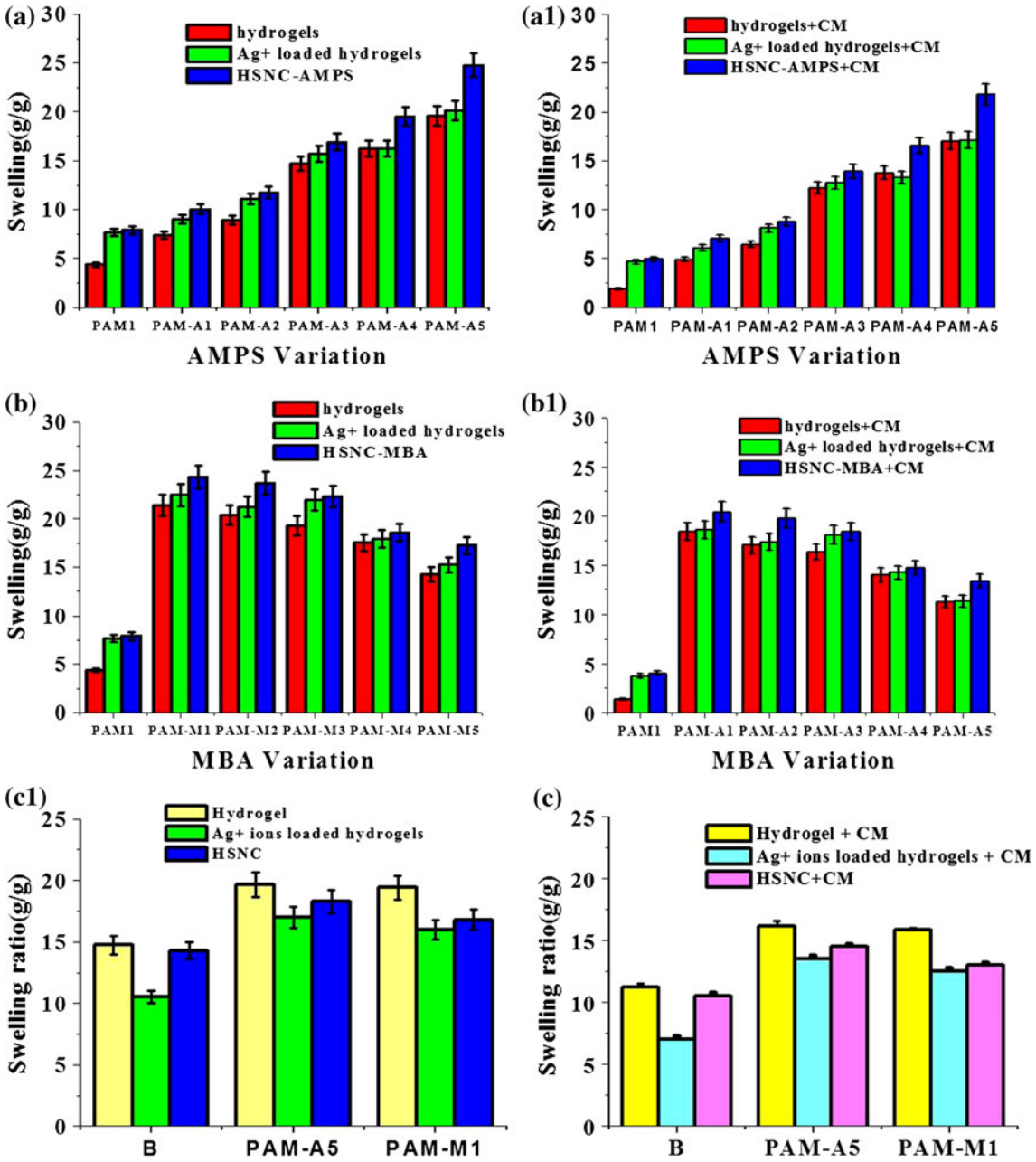

Fig. 1 Swelling pattern of hydrogel, silver ion-loaded hydrogel and HSNC and curcumin loaded HSNC

networks since they have outstanding applications in biological and medical fields. We have designed a simplistic way of producing silver nanoparticles inside the hydrogel networks. The developed nanoparticles exhibit smaller size and finely distributed throughout the hydrogel network.

3.1 Swelling Capacity

The influence of various formulations on the swelling characteristics of hydrogels, hydrogel-loaded silver ions, HSNC and their curcumin loaded hydrogels in water as well as in wound fluids (pseudo extracellular fluids, PECF) were studied in detail. From the Fig. 1, it is confirmed that the reaction parameters such as AMPS and MBA shows significant effect on swelling ratio of hydrogels. Similarly from the Fig. 1a and b it is found that the swelling ratio of hydrogel nanocomposites is higher than that of pure hydrogels and Ag^{+} ions loaded hydrogels. The swelling capacity values was found as hydrogel $<$ Ag^{+} ions loaded hydrogel $<$ HSNC. Almost similar pattern of swelling capacity is also observed for curcumin loaded hydrogels (Fig. 1a1, b1).

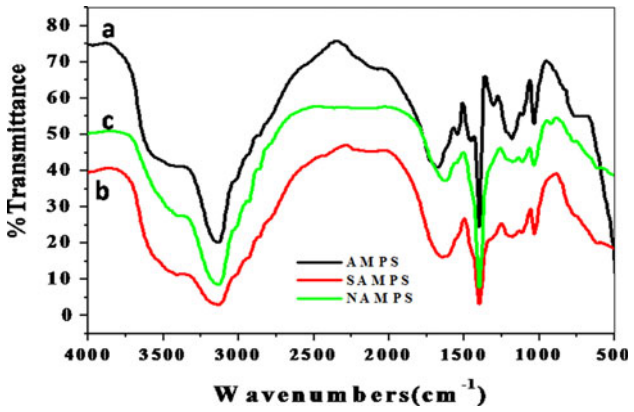

Fig. 2 FTIR spectra of PAM-M3 based hydrogel. *a* Hydrogel *b* Ag^{+} ions loaded hydrogel and *c* HSNC

The swelling behaviour of hydrogels is lower in PECF solution then in water (Fig. 1c). In addition to this the order of swelling capacity also differs i.e. hydrogel > HSNC > Ag^{+} ions loaded hydrogel. This is due to the fact that the ionic strength of the medium influences the swelling capacity of ionic gels. Similar pattern of swelling capacity is also observed for curcumin loaded hydrogels (Fig. 1c1).

3.2 FTIR and UV–Vis spectra analysis

The designed AM and AMPS based hydrogels structure formation can be confirmed by FTIR spectrscopy (Fig. 2). The absorption bands at 3,149 cm^{-1} is attributed due to the –NH stretching vibration of AM unit. The bands at 1675.4

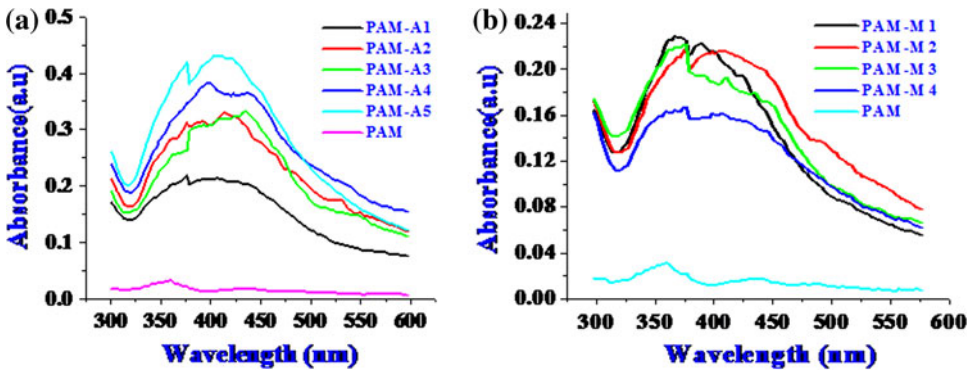

Fig. 3 UV–Vis spectra of the nanoparticles **a** HSNC prepared from hydrogel code PAM and PAM-A1–PAM-A5 **b** PAM and PAM-M1–PAM-M5

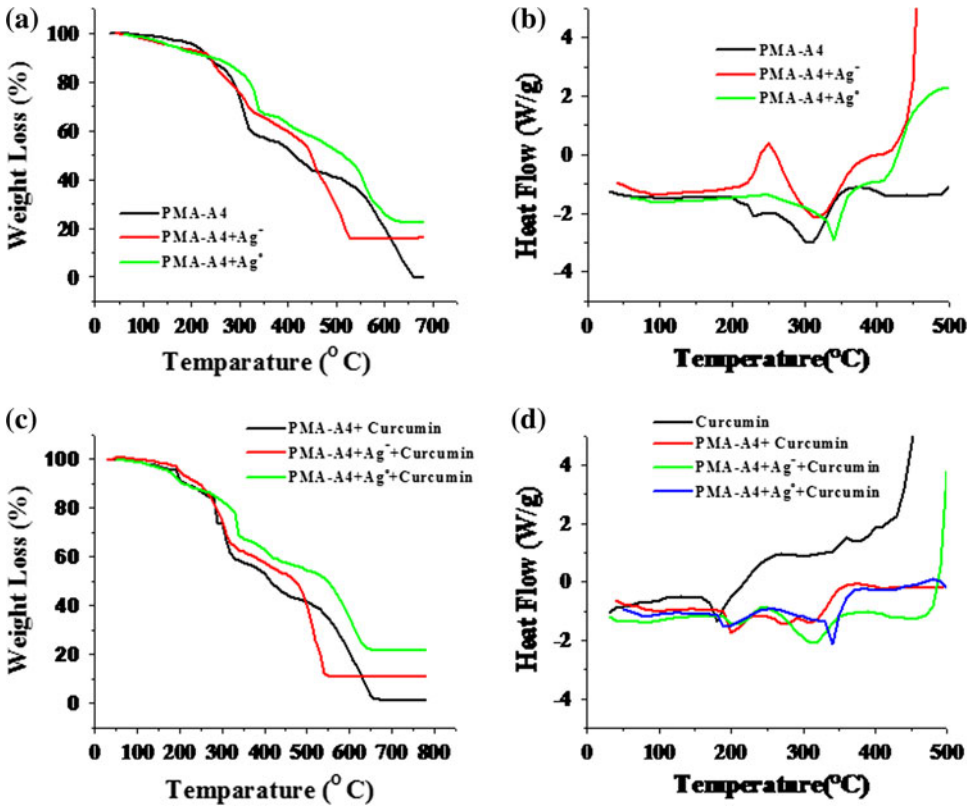

Fig. 4 Thermo gravimetric curves **a** poly(AM-co-AMPS) hydrogel, silver ion loaded hydrogel, and silver nanocomposite hydrogel **c** curcumin loaded silver nanocomposite hydrogels. Differential scanning calorimetric curves **b** plain poly(AM-co-AMPS) hydrogel, silver ion loaded hydrogel and silver nanocomposite hydrogel **d** curcumin and curcumin loaded silver nanocomposite hydrogels

and 1409.5 cm^{-1} indicated the I amide and II amide carboxyl group respectively. The band at 1,202 cm^{-1} represented the C–N stretching vibration of hydrogel units. The absorption band at 1036.4 cm^{-1} is due to the vibrational stretching of the $-SO_3H$ group of AMPS unit [30, 31]. But in the case of Ag^+ loaded hydrogel and HSNC there may be a slight changes in the vibration frequencies (2b, c).The characteristic features of the spectrum of Ag nanoparticle hydrogel composites are all most very similar to those of plain polymer.

The absorption peaks for hydrogel–silver nanocomposites in the 300–600 nm wavelength range in UV–Vis spectra that are assigned to silver nanoparticles which arise from the surface plasmon resonance (SPR). With increase of AMPS concentrations in the HSNC, UV maximum absorbency value also increased (Fig 3a). The reason for this is lower crosslink density as well as an increase in hydrophilic nature to the hydrogel networks with the addition of AMPS. With increase of MBA concentrations, UV maximum absorbency value has decreased (Fig. 3-b).The reason for this is with increase of degree of MBA cross-linking, there is some reduction in the the free volume of the hydrogel networks and thereby less number of silver nanoparticles is formed inside the gel networks.

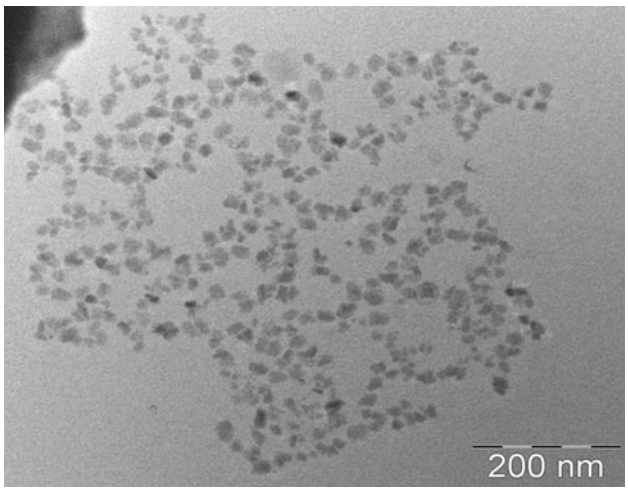

Fig. 5 TEM image of PAM-M3 hydrogel-silver nanocomposite

3.3 Thermal Properties of Hydrogel-Ag NPs-Curcumin Composite

Thermograms of recorded for plain poly(AM-co-AMPS) hydrogel, silver ion loaded hydrogel, silver nanocomposite hydrogel and curcumin loaded silver nanocomposite hydrogels were shown in Fig. 4a and c respectively. From the Fig. 4 it is found that all the three samples starts degrade at 150 °C. At 700 °C 100 %wt loss is noticed for PAM+A4 hydrogel but whereas in PAM-A4+Ag^+ hydrogel 18 % of residue was noticed. But in the case of PAM-A4+Ag^0 hydrogel the more residue is (25 %) noticed which is due to the formation of silver nanoparticles in the hydrogel network. When we observe the thermograms of curcumin loaded hydrogel samples they also shows similar trend as that of bare hydrogels. In addtiton to this curcumin loaded silver nanocomposite hydrogels shows higher thermal stability.

Differential scanning analysis of plain poly(AM-co-AMPS) hydrogel, silver ions loaded hydrogel, silver nanocomposite hydrogel and curcumin loaded silver nanocomposite hydrogels were plotted in Fig 1b and d. DSC of PAM-A4, PAM-A4 Ag^+ and PAM-A4+Ag^0 hydrogels have shown 76.5, 75.2 and 98.4 °C. Formation silver nanoparticles enhance the melting temperature of hydrogel samples. Similarly the curcumin loaded hydrogel samples shows almost similar behaviour. However, because of the presence of curcumin, the curcumin loaded

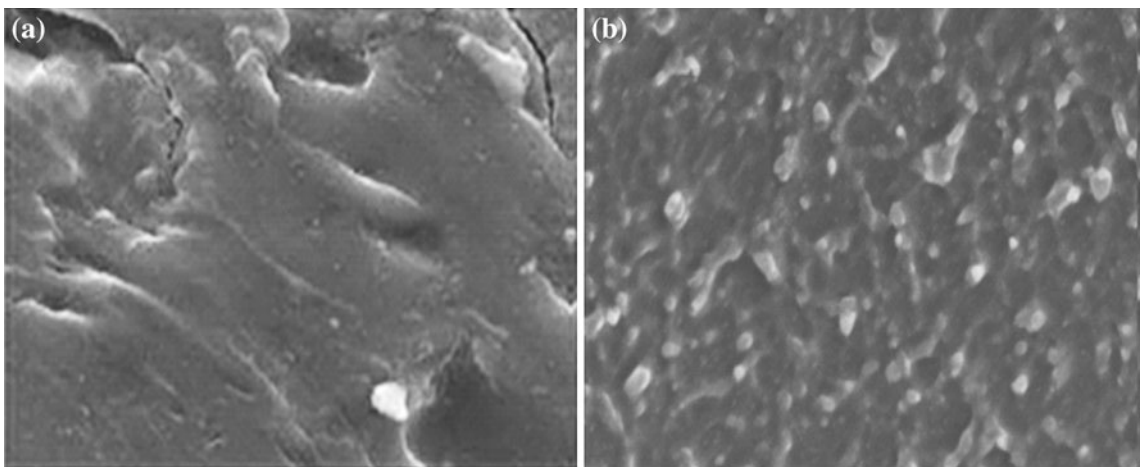

Fig. 6 SEM images of PAM and PAM-M3 HSNC

Table 2 Results of % encapsulation efficiency and % of cumulative releases of placebo hydrogels, silver ions loaded hydrogels and silver nanocomposite hydrogels

Hydrogels code	% of encapsulation efficiency	n	k (10^2)	R^2	% of cumulative releases at 37 °C
P (AM-AMPS) based hydrogels					
PAM-A1	31.14	0.6829	0.9629	0.9334	84.95
PAM-A5	59.47	0.4611	1.3631	0.9386	100
PAM-M1	43.42	0.5323	1.2398	0.9428	96.95
PAM-M5	35.42	0.6436	1.0381	0.9228	84.84
Silver ions loaded hydrogels					
PAM-A1+Ag^+	36.4	0.4998	1.292	0.9285	81.45
PAM-A5+Ag^+	60.2	0.7811	0.817	0.9138	95.8
PAM-M1+Ag^+	45.6	0.5826	1.1558	0.9346	93.15
PAM-M5+Ag^+	37.14	0.75	0.8785	0.898	80.54
Silver nanocomposite hydrogels					
PAM-A1+Ag	61.9	1.0857	0.3918	0.8367	71.57
PAM-A5+Ag	79.2	0.9555	0.619	0.8172	77.95
PAM-M1+Ag	63.42	0.7841	0.8395	0.8886	81.95
PAM-M5+Ag	56.42	1.0407	0.4813	0.8259	74.84

hydrogels have shown an additional peak between 175 and 201 °C due to melting temperature of curcumin.

3.4 Morphology Studies

The morphology of silver nanoparticles were studied by performing electron microscopy analysis. Figure 5 gives the TEM images of the hydrogel nanocomposites. From this image it is found that the nanoparticles are widely aggregated.

SEM images of plain poly(acrylamide-co-acrylamidopropano sulphonic acid) hydrogel and HSNC are depicted in Fig. 6. In Fig. 6a, it is observed that clear and flat surface for pure plain hydrogel. On the other hand silver nanoparticles are clearly visible on the surface of the hydrogel nanocomposite (Fig. 6b).

3.5 Curcumin Loading and Release Studies

The loading efficiency and releasing studies of curcumin into the hydrogels has been examined (Table 2). It is found that the loading efficiency is higher in the case of AgNPs loaded hydrogels compared to other type of hydrogels. The order of loading capacity of curcumin into the hydrogels is found as follows: AgNPs loaded hydrogels > hydrogel > Ag^+ ions loaded hydrogels. The less loading in Ag^+ ions loaded hydrogels is due to all the AMPs chains are bounded by Ag ions and thereby inhibiting the anchoring capacity of drug into the hydrogels.

To understand the drug release from the plain poly (AM-co-AMPS) hydrogel, silver nanocomposite hydrogels and curcumin loaded silver nanocomposite hydrogels, in vitro release experiments were carried out in pH 7.4 buffer solution of at 37 °C. Figure 7 displays the release profiles of different amount of poly(AM-co-AMPS) hydrogel (PAM-A1, PAM-A5 and PAM-M1, PAM-M5) silver nanocomposite hydrogels ((PAM-A1 + Ag^+, PAM-A5 + Ag^+ and PAM-M1 + Ag^+, PAM-M5 + Ag^+) and curcumin loaded silver nanocomposite hydrogels (PAM-A1+Ag^0, PAM-A5+Ag^0 and PAM-M1+Ag^0, PAM-M5+Ag^0) in 7.4 pH media with respect to time. In comparison with the plain poly(AM-co-AMPS) hydrogel, silver nanocomposite hydrogels and curcumin loaded silver nanocomposite hydrogels the plain poly(AM-co-AMPS) hydrogel have faster release, where as curcumin loaded silver nanocomposite hydrogels has shown slower release, This is due to the presence of more number of curcumin molecules that are adsorbed on the silver nanoparticles in addition to the entrapment in the hydrogels. The prolonged release of drug suggests the usefulness of the product towards wound curing for a longer period.

3.6 Antibacterial Activity

The antibacterial activity of the developed the plain poly(AM-co-AMPS) hydrogel, HSNC and curcumin loaded HSNC's were tested against *E. coli* on the nutrient agar medium (Fig. 8). From the Fig. 8a it is observed that the

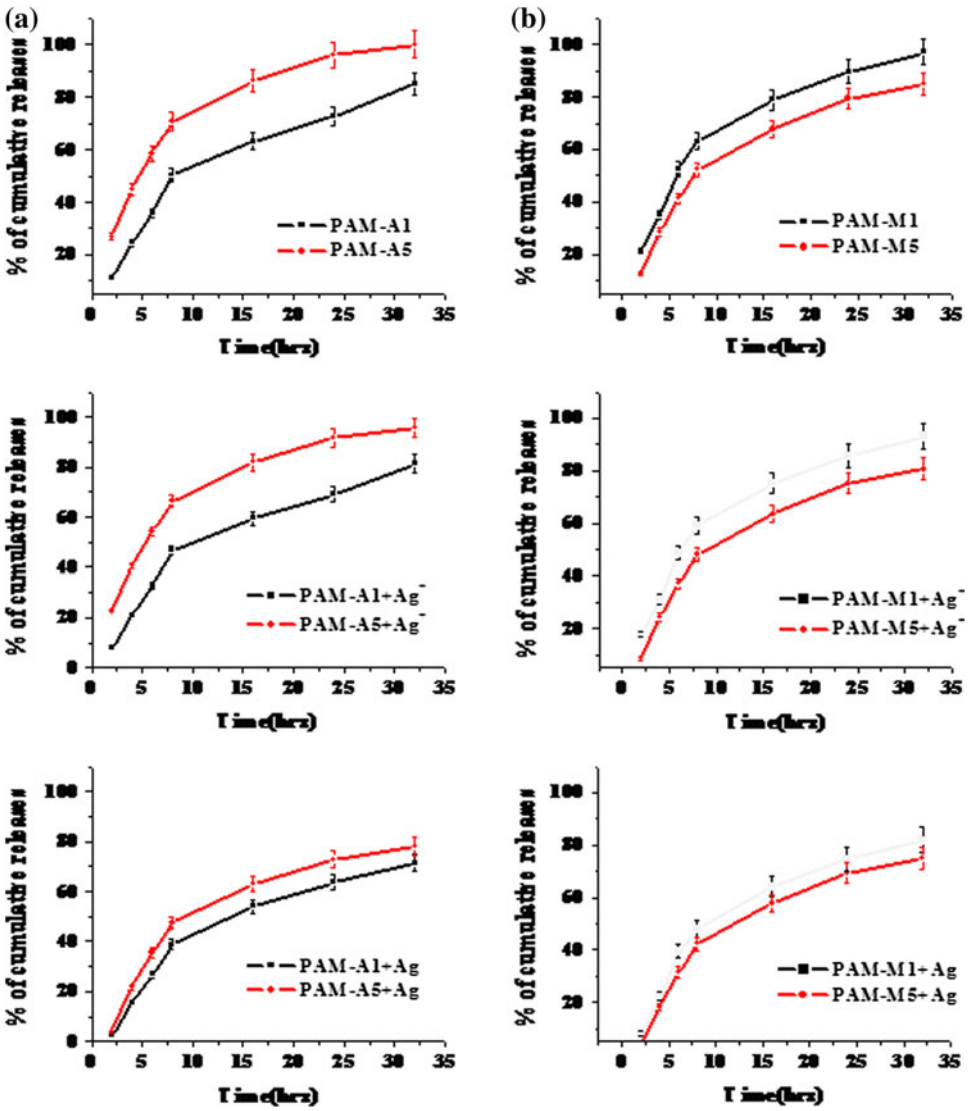

Fig. 7 Cumulative release of curcumin from different hydrogels composites

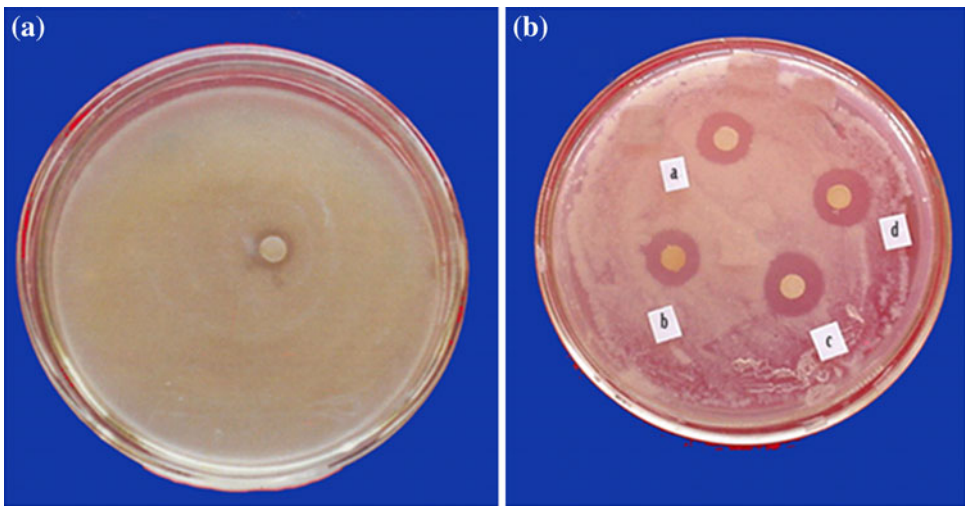

Fig. 8 Photographs showing growth of bacterial colonies in **a** plain poly(AM-co-AMPS) and **b** (*a*) PAM-A1 (*b*) PAM-A5 (*c*) PAM-A5+CM (*d*) PAM-A1+CM

plain hydrogel [poly(AM-co-AMPS)] does not show any effect on the bacterial growth. But both the curcumin loaded HSNC's [(c) PAM-A5+CM (d) PAM-A1+CM)] and HSNC's [(a) PAM-A1 (b) PAM-A5] shows superior bacterial inhibition on the nutrient agar medium than that of pure hydrogel. But within these two nanocomposite hydrogels, curcumin loaded nanocomposites shows well bacterial inhibition. The reason for this is curcumin suppresses the growth of the bacteria and or the release of silver nanoparticles from hydrogel networks Therefore, From these analysis it is conclude that the curcumin loaded HSNC's are excellent antibacterial materials.

4 Conclusions

In summary, a simple and elegant method is adopted to embed the Ag nanoparticles in poly(AM-co-AMPS) hydrogel. For this, a number of poly(acrylamide)/poly (AMPS) hydrogels were formulated by varying the AMPS and MBA concentrations. The formation of silver nanoparticles by poly(AM-co-AMPS) hydrogel networks confirmed by various techniques such as FTIR, UV–Vis, TEM and SEM. The nanoparticles embedded poly(AM-co-AMPS) hydrogel composite exhibits antimicrobial activity against Gram-negative *E. coli*. As a result these nanocomposites can be directly used for antibacterial and wound dressing applications.

Acknowledgments The authors (SR & KMR) thanks the University Grants Commission (UGC-SAP), Government of India, New Delhi for the partial financial support and AFM-B thanks the University of Johannesburg, South Africa for the partial financial support.

References

1. L. Quanroni, G. Chumanov, J. Am. Chem. Soc. **121**, 10642 (1999)
2. S. Chen, J.M. Sommers, J. Phys. Chem. **105**, 8816 (2001)
3. H.A. Clark, P.J. Campagnok, J.P. Wuskell, A. Lewis, L.M. Loew, J. Am. Chem. Soc. **122**, 10234 (2001)
4. S. Shrivastava, T. Bera, A. Roy, G. Singh, P. Ramachandra rao, D. Dash, Nano. Technol. **18**, 225103 (2007)
5. Y. Lu, P. Spyra, Y. Mei, M. Balluff, A. Pich, Macro. Mol. Chem. Phys. **208**, 254 (2007)
6. B. Choi, H. Lee, S. Jin, S. Chun, S. Kim, Nanotechnology **18**(7), 075706 (2007)
7. M.F. Ottaviani, R. Valluzzi, L. Balogh, Macromolecules **35**, 5105 (2007)
8. H.Y. Song, K.K. Ko, I.H. Oh, B.T. Lee, Eur. Cells. mater. **11**, 158 (2006)
9. S.K. Bajpai, Y. Murali Mohan, M. Bajpai, T. Rasika, T. Varsha, J. Nanosci. Nano Technol. **7**, 1 (2007)
10. Y. Gauri, C. Thieulcux, A. Mehdi, C.R. Reye, J.P. Corriu, S. Gomez-Gallardo, K. Philippot, B. Chaudret, Chem. Mater. **15**, 2017 (2003)
11. Y. Plyuto, J.M. Berquier, C. Jacquiod, C. Ricolleau, Chem. Commun. **17**, 1653 (1999)
12. K. Ohno, K. Koh, Y. Tsujii, T.F. Kada, Angew. Chem. Int. Ed. **42**, 2751 (2003)
13. Y. Tan, L. Jiang, Y. Li, D.J. Zhu, Phys. Chem. B. **106**, 3131 (2002)
14. K.S. Mayya, B. Schoeler, F. Caruso, Adv. Funct. Mater. **13**, 183 (2003)
15. J. Tanori, M.P. Pileni, Langmuir **13**, 639 (1997)
16. P. Jain, T. Pradeep, Biotechnol. Bioeng. **90**, 59 (2005)
17. M. Bosetti, A. Masse, E. Tobin, M. Cannas, Biomaterials **23**, 887 (2002)
18. J.F. Hillyer, R.M. Alrecht, J. Pharm. Soc. **90**, 1927 (2001)
19. J. Zuhuang, Patent number C N 1387700 (2003)
20. M. Chen, S. Chen, Patent number C N 1355335 (2002)
21. J.L. Electhiguerra, J.L. Burt, J.R. Morones, A. Camacho-Brabado, X. Gao, H.H. Lara, M.J. Yacaman, J. Nanotechnol. **3**, 1 (2005)
22. C. Wang, N.T. Flynn, R. Langer, Adv. Mater. **16**, 1074 (2004)
23. C. Wang, N.T. Flynn, R. Langer, Mater. Res. Soc. Symp. Proc. **820**, R 2. 2.1 (2004)
24. Y. Lu, P. Spyra, P. Mer, M. Ballauff, A. Pich, Macromol. Chem. Phys. **208**, 254 (2007)
25. P. Saravanan, M.P. Raju, S. Alam, Mater. Chem. Phys. **103**, 278 (2007)
26. H.I. Kima, S.J. Park, S.I. Kim, N.G. Kim, S.J. Kima, Synth. Metals **155**, 674 (2005)
27. R.K. Maheshwari, A.K. Singh, J. Gaddipati, R.C. Srimal, Life Sci. **78**, 2081 (2006)
28. O. Suwantong, P. Opanasopit, U. Ruktanonchai, P. Supaphol, Polymer **48**, 7546 (2007)
29. S.Y. Lin, K.S. Chen, Run-Chu L, Biomaterials. **22**, 2999 (2001)
30. A.A.A. Abdel-Azim, M.S. Farahat, A.M. Atta, A.A. Abdel-Fattah, Polym. Adv. Technol. **9**, 282 (1998)
31. C. Zhang, A.J. Easteal, J. Appl. Polym. Sci. **88**, 2563 (2003)